Self-assembly of one-dimensional nanomaterials for cost-effective photovoltaics

Zhiyong Fan*

Department of Electronic and Computer Engineering,
Hong Kong University of Science and Technology,
Clear Water Bay, Kowloon, Hong Kong
E-mail: eezfan@ust.hk

Johnny C. Ho*

Department of Physics and Materials Science,
City University of Hong Kong,
Tat Chee Avenue, Kowloon, Hong Kong
E-mail: johnnyho@cityu.edu.hk
*Corresponding authors

Abstract: As the demand for sustainable energy resources has grown rapidly in recent years, enormous effort is invested on cost-effective photovoltaic technologies. Nanomaterials are one class of candidate materials being explored for next generation photovoltaics while significant progress has been obtained currently. In this review article, we summarise the recent progress in this field and identify the key issues related to nanostructured solar cells. In particular, we highlight the technology which is based on self-assembly of synthetic nanopillars for photovoltaics. These research has casted a solid ground for future exploration using nanomaterials for cost-effective solar cells.

Keywords: photovoltaics; PVs; nanopillars; NPLs; light trapping; carrier collection; low cost; flexible solar cells.

Reference to this paper should be made as follows: Fan, Z. and Ho, J.C. (2011) 'Self-assembly of one-dimensional nanomaterials for cost-effective photovoltaics', *Int. J. Nanoparticles*, Vol. 4, Nos. 2/3, pp.164–183.

Biographical notes: Zhiyong Fan received his BS and MS in Physical Electronics from Fudan University, China. He then received his PhD in Materials Science from University of California, Irvine in 2006. From 2007 to 2010, he worked in University of California, Berkeley as a Postdoctoral Fellow in the Department of Electrical Engineering and Computer Sciences, with a joint appointment with Lawrence Berkeley National Laboratory. In May 2010, he joined Hong Kong University of Science and Technology as an Assistant Professor. His research interest rests in synthesis of functional nanomaterials and their applications for electronics, sensing and energy harvesting.

Johnny C. Ho obtained his BS in Chemical Engineering with high honours from University of California at Berkeley in 2002. He then received his MS and PhD in Materials Science and Engineering from University of California at Berkeley in 2005 and 2009, respectively. Before beginning his academic position at City University of Hong Kong, he performed studies on energy-harvesting devices as a Post-doctoral Fellow at Lawrence Livermore

National Laboratory, California. His research interest is highly interdisciplinary involving chemistry, physics, materials science and various engineering disciplines to explore novel nanomaterials and nano-engineering techniques for technological applications.

1 Introduction

In the past decade, one-dimensional (1D) and quasi-one-dimensional (Q-1D) materials, including nanowires (NWs), nanorods (NRs), and nanopillars (NPLs), have been extensively studied as the novel building materials for a broad range of applications such as electronics (Ford et al., 2009; Thelander et al., 2008; Javey, 2008; Lu and Lieber, 2007; Javey et al., 2007; Xiang et al., 2006; Wang and Dai 2006), optoelectronics (Qian et al., 2005; Fan et al., 2004a; Zhong et al., 2003), and sensors (Chen et al., 2008; Fan et al., 2008a, 2004b; Zhang et al., 2004; Fan and Lu, 2005; Hahm and Lieber, 2004), etc. Not until recently, as an emerging field, this new class of nanomaterials has been utilised for building energy conversion/harvesting devices, to convert mechanical (Wang and Song 2006), thermal (Hochbaum et al., 2008; Hasegawa et al., 2009), and solar energy into electricity (Fan et al., 2009; Czaban et al., 2009; Garnett and Yang, 2008; Kempa et al., 2008; Colombo et al., 2009; Tang et al., 2008; Kelzenberg et al., 2008; Martinson et al., 2008; Tian et al., 2007; Tsakalakos et al., 2007; Law et al., 2005; Song et al., 2005). Particularly, for photovoltaic (PV) applications, synthetic 1D semiconductors are typically grown with low-cost 'bottom-up' approaches with the high crystallinity, ensuring the superb electrical carrier transport. In addition, arrays of 1D nanomaterials can further improve photon absorption utilising light trapping effect (Fan et al., 2010); therefore, a combination of these figures of merit can lead to next generation PV devices with great cost-effectiveness. In this review article, we summarise the recent progress of 1D/Q-1D nanomaterials-based PV research followed by a perspective of the future development of this technology.

2 Single NW PV devices

Studies on PV effect from single NW devices constitute the fundamentals of the practical PV technologies with nanostructures and nanomaterials. In this regard, ground-breaking work on single NW PV devices has been performed by a few pioneers. For example, Si NWs with the axial *p-i-n* junction structure have been successfully grown with vapour phase catalytic method in conjunction with the in-situ doping modulation technique (Kempa et al., 2008; Tian et al., 2007). Similar to thin film amorphous silicon *p-i-n* solar cells, the intrinsic segments of Si NWs are the photosensitive region which generates electron-hole pairs (EHPs). It was found that the longer intrinsic region resulted in the higher conversion efficiency. An optimal PV device [Figure 1(a), inset] based on this type of NW has been demonstrated with an open circuit voltage (V_{oc}) around 0.29 V [Figure 1(a)], a short circuit current density (J_{sc}) of 3.5 mA/cm^2, and a maximum conversion efficiency of 0.5% (Kempa et al., 2008). One step further, axial tandem

p-*i*-n^+-p^+-*i*-*n* NW PV devices have been fabricated with the same growth approach to achieve the increased V_{oc}, as shown in Figure 1(b) (Kempa et al., 2008).

Single NW solar cells with axial junctions showed relatively low conversion efficiency mainly due to the fact that the direction of carrier transport is along the long axis of NWs, and the large surface area of NWs results in significant surface recombination. As compared to the axial junction structure, the radial junction structure has been considered as a more promising structure for NW PV devices since the minority carrier collection/transport is along the radial direction, thus greatly shortens the carrier travel and improves the collection efficiency (Garnett and Yang, 2008; Tian et al., 2007; Kayes et al., 2005). Experimentally, radial *p*-*i*-*n* NW structures have been fabricated with Si, GaAs, etc. (Kempa et al., 2008; Colombo et al., 2009; Tian et al., 2007). In a representative work, a Si single NW *p*-*i*-*n* structure was grown using a Au catalysed vapour-liquid-solid (VLS) method with silane, diborane, and phosphine as the Si source, *p*-type and *n*-type dopant, respectively. This core-shell NW is consisted of a *p*-type NW core with an intrinsic and *n*-type shell. The *p*-type core was single crystalline, while the shells were polycrystalline with grain size of 30–80 nm. A PV device can be fabricated with electron-beam lithography (EBL) followed by the shell etching and metallisation. The scanning electron microscopy (SEM) image of a typical device is shown in Figure 1(c). Figure 1(d) demonstrates the dark and light *I*-*V* curves measured for a corresponding core-shell NW PV device. From dark measurements, it was found that both diode ideality factors and reverse bias breakdown voltages were significantly improved upon insertion of an intrinsic Si layer which also agrees with the observation in the axial *p*-*i*-*n* NW case (Tian et al., 2007). The illuminated (light) curves from such devices were measured under AM 1.5G. And an open circuit voltage of 0.26 V, a short circuit current of 0.503 nA, and a fill factor of 55% were measured, corresponding to a maximum power output of ~72 pW under 1 sun and device conversion efficiency ~3.4% after exclusion of the metal covered area, which is 7× improved from the axial *p*-*i*-*n* NW PV device.

To further shed light on the efficiency loss mechanism, temperature dependent measurements were performed on illuminated NWs (Kempa et al., 2008). Reduced temperatures produced a small decrease in I_{sc}, attributed to the increasing band-gap energy, and a linear increase in V_{oc} which is in close agreement with the value found for planar single crystalline Si solar cells. Reduced carrier recombination at lower temperatures was suggested as the mechanism responsible for this linear increase in V_{oc}. Meanwhile an increase in the fill factor with decreasing temperatures was also observed. The result showed an improved efficiency up to 6.6% at 80 K under 0.6-sun illumination. While the ongoing solar cell operation at 80 K is not practical, this study suggested that significant performance improvements are available by further reducing carrier recombination through other methods, such as improvements to the morphology of the NW shells, the core-shell interfaces, and passivation of the shell surfaces and grain boundaries.

Although Si is the dominant material for conventional planar solar cells and radial *p*-*i*-*n* Si NW cells have been demonstrated for better efficiency than the axial *p*-*i*-*n* ones, due to the relative low optical absorption coefficient, Si may not be the ideal material for single NW solar cells with the configuration horizontally lying on substrates for their small diameters. In comparison, GaAs has a much higher optical absorption coefficient and close to the ideal energy band-gap (E_g = 1.45 eV), thus has a promising potency for efficient NW solar cells. It has been reported that radial *p*-*i*-*n* GaAs NW PV devices can

also be fabricated (Colombo et al., 2009). The structure of the NW and contact geometry were similar to the aforementioned coaxial Si PV devices, except that NWs were fabricated by molecular beam epitaxy (MBE) without relying on Au catalysts, to ensure the high quality interface and avoid the metallic impurity. The NWs also had a *p*-type core, intrinsic and *n*-type shells structure using Si as both the *n*- and *p*-type dopants. Si can be used as a *n* or *p*-type dopant in GaAs depending on whether it occupies Ga or As sites, respectively, though additional work is necessary to elucidate the mechanism and conditions responsible for this doping behaviour. Typically, a NW length of 9 μm and thicknesses of the intrinsic and *n*-type shells of 15 nm and 50 nm, respectively, were obtained. And PV devices were fabricated using EBL similar to the Si ones.

Figure 1 Single NW PV device (a) illuminated *I-V* characteristics for the i-length = 0, 2, and 4 μm devices* (b) *I-V* responses measured on p-i (2 μm) -n (red) and *p-i-n*+-*p*+-*i-n*, *i* = 2 μm (blue)** (c) an SEM image corresponding to the NW device schematic of metal contacts deposited on the p-core and n-shell*** (d) dark and illuminated *I-V* curves (see online version for colours)

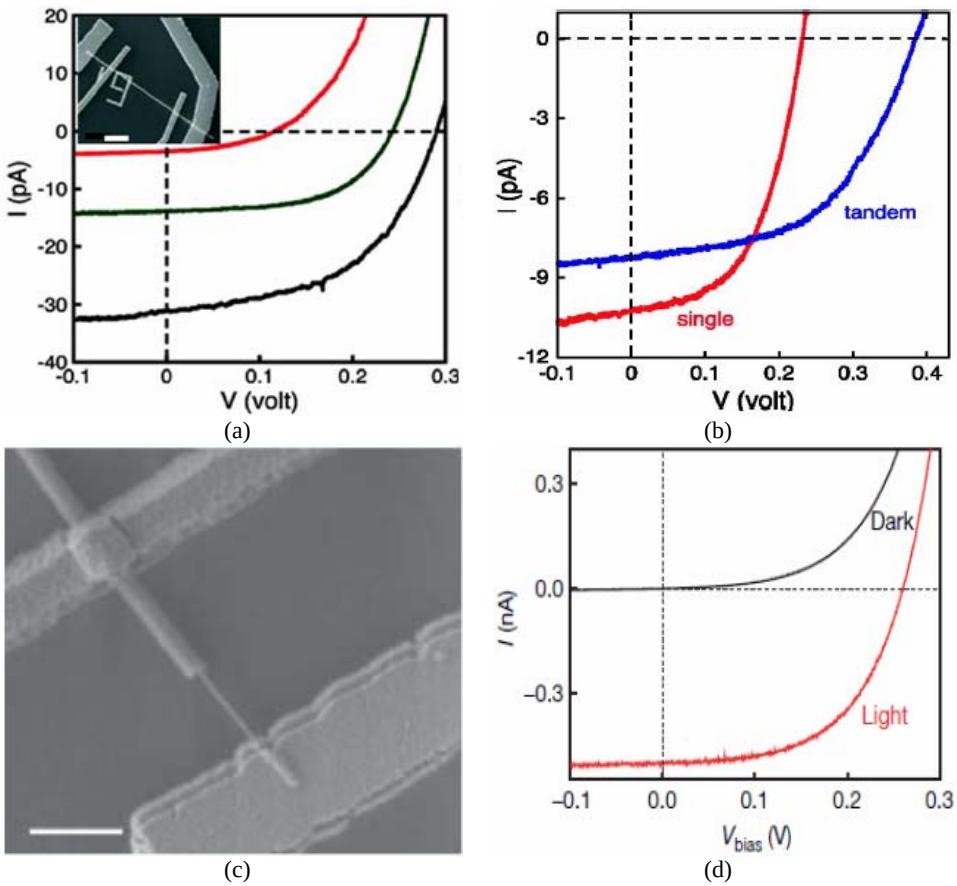

Notes: *The illumination intensity was 100 mW/cm^2, AM 1.5G (insert: SEM image of a *p-i-n* SiNW device with the i-length of 2 μm; scale bar is 4 μm); **SiNW devices under AM 1.5G illumination; *** scale bar is 1.5 μm.

Source: Reprinted with permission from Kempa et al. (2008) and Tian et al. (2007)

To evaluate the device performance, *I-V* curves were acquired under light intensity ranging from dark to 200 μW power with the best performed device producing an efficiency of 4.5% and a fill factor of 0.65 under AM 1.5 illumination at room temperature.

3 NW arrays for PVs

Studies of single NW PV devices provide us with fundamental understanding of the nanoscale PV effect. Meanwhile, these nanoscale solar cells can be potentially used to drive the nanoelectronic components (Tian et al., 2007). Nevertheless, the need for large-scale and affordable solar cell modules and panels appear to be more urgent for the sake of environmental sustainability. In this regard, developing scalable and affordable PV technologies with nanostructures and nanomaterials is of the paramount importance, for researchers working in the field of nanotechnology.

As compared to bulk and thin film materials, synthetic nanomaterials can be grown at much lower temperature than the bulk in order to get single crystalline structures (Mohammad, 2009; Fan et al., 2008b; Wang et al., 2006). This can help to reduce material extraction cost dramatically. On the other hand, nanostructured materials have unique favourable properties for PV that the bulk and thin film materials do not possess, such as the much improved light absorption capability and carrier collection efficiency, as these will be discussed in the following paragraphs.

3.1 Engineering light absorption with 3D structures

In general, the energy conversion efficiency of a solar cell device depends on primarily two processes: absorption of the incident photons and the subsequent collection of the photo-generated carriers. From the optical absorption point of view, arrayed NWs, NRs and NPLs with the 3D configuration can provide a unique anti-reflection mechanism to improve the optical absorption (Zhu et al., 2009; Muskens et al., 2008). This anti-reflection mechanism can be simply referred to the light trapping effect, or structurally tuned refractive effective index gradient (Stiebig et al., 2006). There have been a number of materials configured as 3D nanostructures, including Si (Kelzenberg et al., 2010), Ge (Fan et al., 2010), CdS (Fan et al., 2009), etc. Extensive work has been done on the optical properties of Si NW arrays (Kempa et al., 2008; Kelzenberg et al., 2008). For example, as shown in Figure 2(a), Si wire arrays were grown by a photolithographically patterned VLS process on p-type <111> Si wafers and evaporated Au, Cu or Ni were used as the catalyst (Kelzenberg et al., 2010). As shown in Figure 2(b), a much improved absorption spectrum can be achieved on Si wire arrays. It was observed that with less than 5% areal fraction of wires, up to 96% peak absorption could be achieved leading to absorption of 85% of the day-integrated, above-bandgap direct sunlight (Kelzenberg et al., 2010). In addition, these arrays showed an improved near-infrared absorption, which allows overall sunlight absorption to exceed the ray-optics light-trapping absorption limit for an equivalent volume of randomly textured planar Si over a broad range of incidence angles.

Figure 2 Nanostructures with enhanced light absorption (a) a SEM image of a peeled-off* (b) illustration of the normal-incidence** (c) average absorption efficiency*** (d) cross-sectional SEM images**** (see online version for colours)

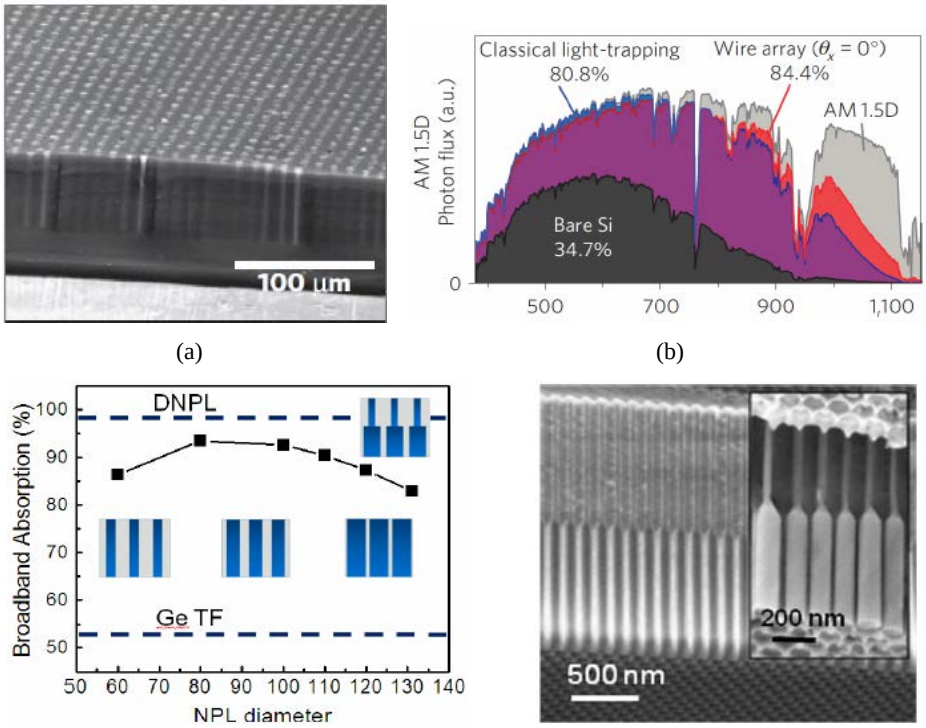

Notes: *Polymer-embedded wire array, viewed upside-down (at 60° tilt) to illustrate the order and fidelity of the embedded wires; **spectrally weighted absorption of the AM 1.5D reference spectrum, corresponding to each of the three absorption cases: Si wire array which had an equivalent planar Si thickness of 2.8 µm, a 2.8-µm-thick planar Si absorber, with an ideal back-reflector, assuming: bare, non-texturised surfaces and ideally light-trapping, randomly textured surfaces; ***over λ = 300–900 nm for single-diameter NPLs as a function of diameter along with that of a DNPL array with D1 = 60 nm and D2 = 130 nm; ****of a blank AAM with dual-diameter pores and the Ge DNPLs (inset) after the growth.

Source: Reprinted with permission from Kelzenberg et al. (2010) and Fan et al. (2010)

In another work, rather than using the lithographic method and epitaxial wafer to obtain regular arrays of wire, Ge NPLs were assembled in the anodic alumina membrane (AAM) via the vapour phase catalytic growth method (Fan et al., 2009). By varying the diameter, pitch, length of the pores, the shape of Ge NPLs can be well controlled. Transmission electron microscopy (TEM) investigation showed that the grown NPLs are single crystalline which highly favours the carrier transport. Optical reflectance/transmission measurements showed that with the fixed pitch, NPL arrays with the large NPL diameter has high reflectance but low transmission, and NPL arrays with the small NPL diameter has the opposite effect. As a result, there existed an optimal

diameter which yielded a maximal 94% broad-band light absorption, as shown in Figure 2(c). Compared to the Ge blank film with only ~53% broad-band light absorption; a Ge NPL array has already achieved a much improved optical absorption. To further improve this figure of merit, a unique dual-diameter NPL (DNPL) structure [Figure 2(d)] was fabricated by simply multiple-step etching and anodisation (Fan et al., 2010). Utilising high transmission of a small diameter structure and high absorption from a large diameter structure, an optimal DNPL array has achieved ~99% broad-band optical absorption (Fan et al., 2010).

Figure 3 Nanostructures with enhanced carrier collection (a) radial-junction NR solar cells* (b) spectral response of typical photoetched planar and NR array** (c) conversion efficiencies of the SNOP and planar cells versus the minority carrier (electron) diffusion length of the CdTe film*** (see online version for colours)

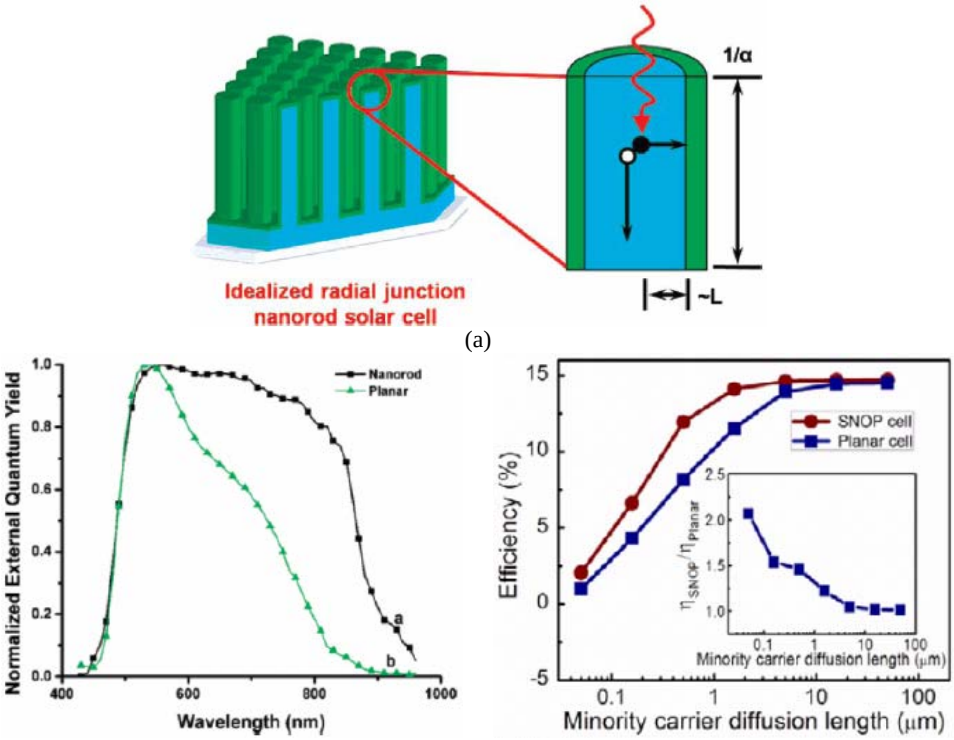

Notes: *Do not require the collection length to be this long because they can absorb light in the axial direction while collecting charge carriers in the radial direction. This schematic diagram is not to scale; **photoelectrochemical cells with the external quantum yield normalised to its highest value. The quantum yield of the NR array electrodes at wavelengths greater than 600 nm decreased less than that of the planar electrodes. The black solid line with squares (a) is the normalised spectral response of the NR array electrode, and the green solid line with triangles (b) is the normalised spectral response of the planar electrode; ***the total device thickness is fixed at 1.3 μm concluding electrodes. The inset shows their ratio, depicting the advantage of SNOP-cell, especially when the minority carrier life times are relatively low.

Source: Reprinted with permission from Spurgeon et al. (2008) and Fan et al. (2009)

3.2 Carrier collection improvement

Besides improving the optical absorption, using arrays of NWs and NPLs as active PV materials can also enhance the photo-carrier collection efficiency if the structure is properly designed. For the thin film type of solar cells, it is well known that in order to achieve high efficiency, the material has to be thick enough to absorb majority part of the incident photons. However, if the material is polycrystalline or even amorphous with the relatively short minority carrier diffusion length, thick material can be detrimental for carrier collection. Thus, optical absorption and carrier collection are in competition in thin film devices and fabricating low-cost films that simultaneously absorb photons and collect carriers efficiently is challenging. In this regard, many NW solar cell architectures offer the advantage of orthogonalising the light absorption and carrier collection directions (Fan et al., 2009; Kelzenberg et al., 2010; Spurgeon et al., 2008) as shown in Figure 3(a), which can relax the competition between photon absorption and carrier collection. In fact, a comparison between NR arrays and planar Cd (Se, Te) photoelectrodes has been made (Spurgeon et al., 2008). It was shown that the fill factors of the NR array photoelectrodes were superior to those of the planar junction devices. More importantly, the spectral response of the NR array photoelectrodes exhibited better quantum yields for collection of near-IR photons relative to the collection of high-energy photons than the planar photoelectrodes, as shown in Figure 3(b).

The performance benefit of orthogonalising photon absorption and carrier collection is also demonstrated with the simulation of the CdS NPL/CdTe thin film hybrid solar cells (Fan et al., 2009). In this work, the conversion efficiency of a device structure consisting of CdS NPL arrays embedded in a CdTe thin film were compared to that of a planar CdS/CdTe cell. The NPL structure showed the better conversion efficiency than its thin film counterpart, especially for small minority carrier diffusion lengths, as shown in Figure 3(c). This result provides an important guideline for solar cell design using low cost and low grade materials.

4 Materials for nanostructured PVs

Up-to-date, there have been a number of work reporting NW, NR, NPL array-based PV devices using ZnO, Si, GaAs, etc. as active materials (Fan et al., 2009; Colombo et al., 2009; Kelzenberg et al., 2010; Garnett and Yang, 2010; Greene et al., 2007; Law et al., 2006). Figure 4(a) and Figure 4(b) demonstrate a pioneering work using ZnO NW arrays for dye-sensitised solar cells (Law et al., 2005). In this work, vertical arrays of ZnO NWs were grown on F:SnO2 (FTO) substrates, as shown in Figure 4(a). The electron diffusivity within the wires was estimated to be between 0.05–0.5 $cm^2\ s^{-1}$, much higher than that estimated for typically used ZnO nanoparticle films. PV measurements showed device characteristics of a short circuit current density, J_{sc} = 5.3–5.85 mA cm^{-2}, open circuit voltage, V_{oc} = 0.61–0.71 V, fill factor, FF = 0.36–0.38 and the resulting efficiency, η = 1.2%–1.5% as plotted in Figure 4(b). The highest external quantum efficiency of the cell measured [Figure 4(b) Inset] was 40% at 515 nm wavelength, corresponding to the maximum absorption of the dye. The efficiency of the dye sensitised solar cell can be further improved by maximising photon absorption at higher wavelengths in increasing the length of the cell, if electron diffusion length can be increased at the same time. In this regard, one simple method to increase electron diffusion lengths is through reducing

the interfacial recombination rate by applying surface coatings on the nanocrystalline film (Bandaranayake et al., 2004; Diamant et al., 2004; Palomares et al., 2003; Tennakone et al., 2001; Zaban et al., 2000). For example, a conformal layer of TiO_2 was deposited on ZnO NWs via an atomic layer deposition system (Law et al. 2005). This oxide shell is expected to suppress recombination by incorporating an energy barrier that physically separates the photo-generated electrons from the oxidised species within the electrolyte. The layer also acts to passivate the recombination centres on the surface of the NWs. The results showed an overall conversion efficiency of 2.25%, a significant improvement in performance of the cells.

Figure 4 Representative NW array PV (a) typical SEM cross-section of a cleaved NW array on FTO* (b) traces of current density against voltage (*J-V*) for two cells with roughness factors of ~200** (c) tilted cross-sectional SEM of the completed ordered silicon NW radial*** (d) solar cell output characteristics**** (see online version for colours)

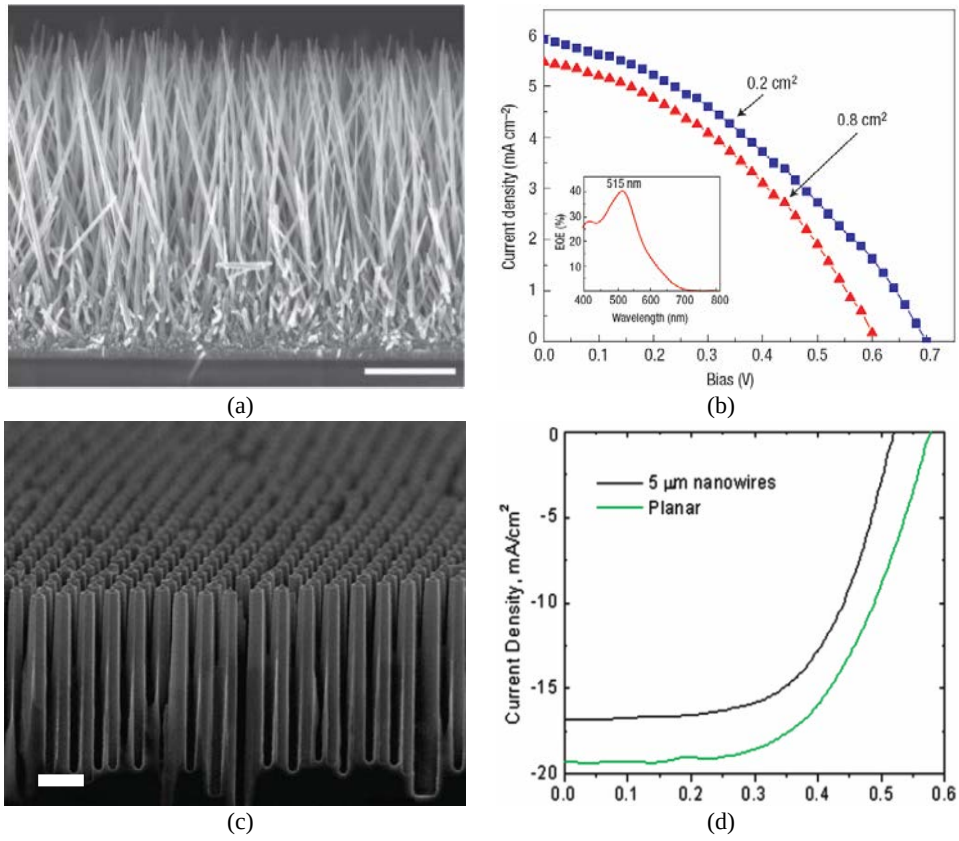

(a) (b) (c) (d)

Notes: *The wires are in direct contact with the substrate, with no intervening particle layer. Scale bar = 5 μm; **the small cell (active area: 0.2 cm^2) shows a higher *Voc* and *Jsc* than the large cell (0.8 cm^2). The fill factor and efficiency are 0.37% and 1.51% and 0.38% and 1.26%, respectively. Inset shows the external quantum efficiency against wavelength for the large cell; ***p-n junction array solar cell made by bead assembly and deep reactive ion etching. Scale bar = 1 μm; ****for 5 μm NWs and planar control solar cells fabricated from a 25 μm thin silicon absorber.

Source: Reprinted with permission from Law et al. (2005) and Garnett and Yang (2010)

As the second most abundant element in earth's crust, Si is the dominant material for microelectronics, as well as PVs. Till now, Si-based nanostructure solar cells have still attracted enormous attention (Garnett and Yang, 2008, 2010; Kempa et al., 2008; Tian et al., 2007; Kelzenberg et al., 2010). Figure 4(c) demonstrates an arrayed Si NW solar cell on the *n*-type Si wafer. The NW array was achieved by self-assembly of silica spheres on the wafer followed by the deep reactive ion etching (Garnett and Yang 2010). Then the boron diffusion was performed on samples to produce radial *p*-*n* junctions. Note that this approach ensured that NWs are single crystalline; more importantly, NWs were not fabricated with the metal catalyst, thus, avoiding metallic contamination which introduced deep level trapping states and shorten minority carrier life-times (Bullis, 1966). As the result, an energy conversion efficiency of about 5.3% was achieved, which is increased by 22% over the planar control sample. This improvement was also attributed to the strong light trapping effect from the 3D structure.

Although Si and GaAs NW arrays have been extensively explored for PV studies, they have relatively high surface recombination velocities, which degrade the cell conversion efficiency by the significant carrier surface recombination. Specifically, the reported surface recombination velocities of both non-passivated planar silicon and gallium arsenide structures have exceeded 10^6 cm s^{-1} making these materials unsuitable for the NW arrays solar cell configuration (Sharma et al., 2007; Sabbah and Riffe, 2000; Rowe et al., 1993; Passlack et al., 1996; Jastrzebski et al., 1975). On the other hand, II-VI compound semiconductors are notable for their relatively low untreated surface recombination velocities, typical cadmium sulphide (CdS) and cadmium telluride (CdTe) thin films have the untreated surface recombination velocities around 10^3 and 10^4 cm s^{-1}, respectively, which make these material systems favourable for solar cells in this case (Rosenwaks et al., 1990; Delgadillo et al., 1997).

5 CdS/CdTe solar nanopillar (SNOP) cells

In this regard, Fan et al. (2009) reported a recent work on NPL array solar cells utilising the CdS/CdTe material system which demonstrated the versatility of NW-based PVs. Notably, this work employed a novel technique to fabricate single crystalline semiconductor materials non-epitaxially on amorphous substrates. Using the template assisted synthesis, highly ordered NPL arrays were obtained to enable cost-effective fabrication of crystalline solar cell modules. Moreover, the *n*-type CdS NPL arrays embedded in a p-type CdTe thin film resulting in a three-dimensional (3D) structures, which took full advantage of the orthogonal relationship between photon absorption and carrier collection previously discussed. Compared to the conventional planar cell structures, relying on the optical generation and separation of EHPs with an internal electric field, this SNOP structure enhances the photocarrier separation and collection by orthogonalising the direction of light absorption and EHPs separation (Spurgeon et al., 2008; Hu and Chen, 2007; Tsakalakos et al., 2007; Kayes et al., 2005; Fahrenbruch and Bube, 1983). This distinguished difference relieved the competition between absorption and carrier collection and opened the design space for cost competitiveness and further exploration.

A simple process schematic of the NPL solar cells is depicted in Figure 5. In general, a 2 μm thick alumina film was grown on a 0.25 mm thick aluminium foil by anodisation

in phosphoric acid solution at low temperature (~5°C). Highly ordered pores in the alumina membrane formed a hexagonal array with the controlled pitch and pore diameter while the ordering was achieved by a combination of a pre-anodisation nanoimprint on the aluminium foil and matching the nanoimprint pitch with a proper anodisation voltage (Mikulskas et al., 2001; Masuda et al., 1997), Figure 6(a) shows a SEM image of an AAM with the long-range and near-perfect ordering after the anodisation process. A barrier-thinning step was utilised to broaden the pore channels and reduce the alumina barrier layer thickness at the bottom of the pores to a few nanometres. Thinning the barrier allowed for the electrodeposition of Au selectively at the bottom of the pores and this Au layer later acted as the catalyst for the CdS NPL synthesis via the VLS growth mode. The processed AAM was partially and controllably etched in 1N sodium hydroxide solution (NaOH) at room temperature to expose the tips of the pillars to form the 3D structures [Figure 6(b)]. Importantly, this etching solution is highly selective and does not chemically react with and degrade the material quality of CdS NPLs. Also, the exposed depth could be varied and controlled by adjusting the etching time to optimise the geometric configuration, where the device thickness comparable to the optical absorption depth and the bulk minority carrier diffusion length, for the enhanced conversion efficiency. After that, a p-type CdTe thin film with ~1 μm thickness was then deposited by chemical vapour deposition to serve as the photoabsorption layer due to its optimal band-gap (Eg = 1.5 eV) for the solar energy absorption (Fahrenbruch and Bube, 1983). The top electrode was finally deposited by the thermal evaporation of Cu/Au (1 nm/13 nm) in order to achieve an acceptable transparency and to form an ohmic contact with the *p*-type CdTe film. In future, further top-contact optimisation is required to explore the transparent conductive contacts, such as indium tin oxide (ITO), etc. The backside electrical contact to the n-type CdS NPLs was simply the aluminium support substrate while the entire solar cell device could then be bonded on the top to a glass slide by epoxy for the encapsulation.

Figure 5 CdS NPLs/CdTe thin film cell fabrication scheme (a) anodic alumina membrane* (b) template-assisted VLS growth of CdS NPLs is then applied (c) AAM is partially etched to expose the top of the NPLs (d) thin film of CdTe is deposited on the exposed NPL array by CVD** (see online version for colours)

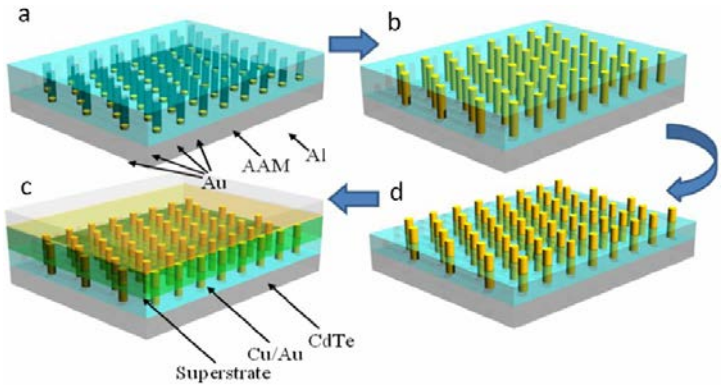

Notes: *AAM is grown on aluminium foil to form an array of pores in which Au catalyst is electrochemically deposited at the bottom; **followed by thermal evaporation of Cu/Au top contact.

Source: Reprinted with permission from Fan et al. (2009)

Figure 6 Characterisation of CdS NPLs (a) SEM image of highly ordered alumina pores used as the template for the VLS growth of CdS NPLs (b) SEM image of partially exposed CdS NPLs in AAM (c–d) TEM image verifying the single crystallinity of the CdS NPLs (e) TEM demonstrates the abrupt junction at the CdS NPL/CdTe thin film interface

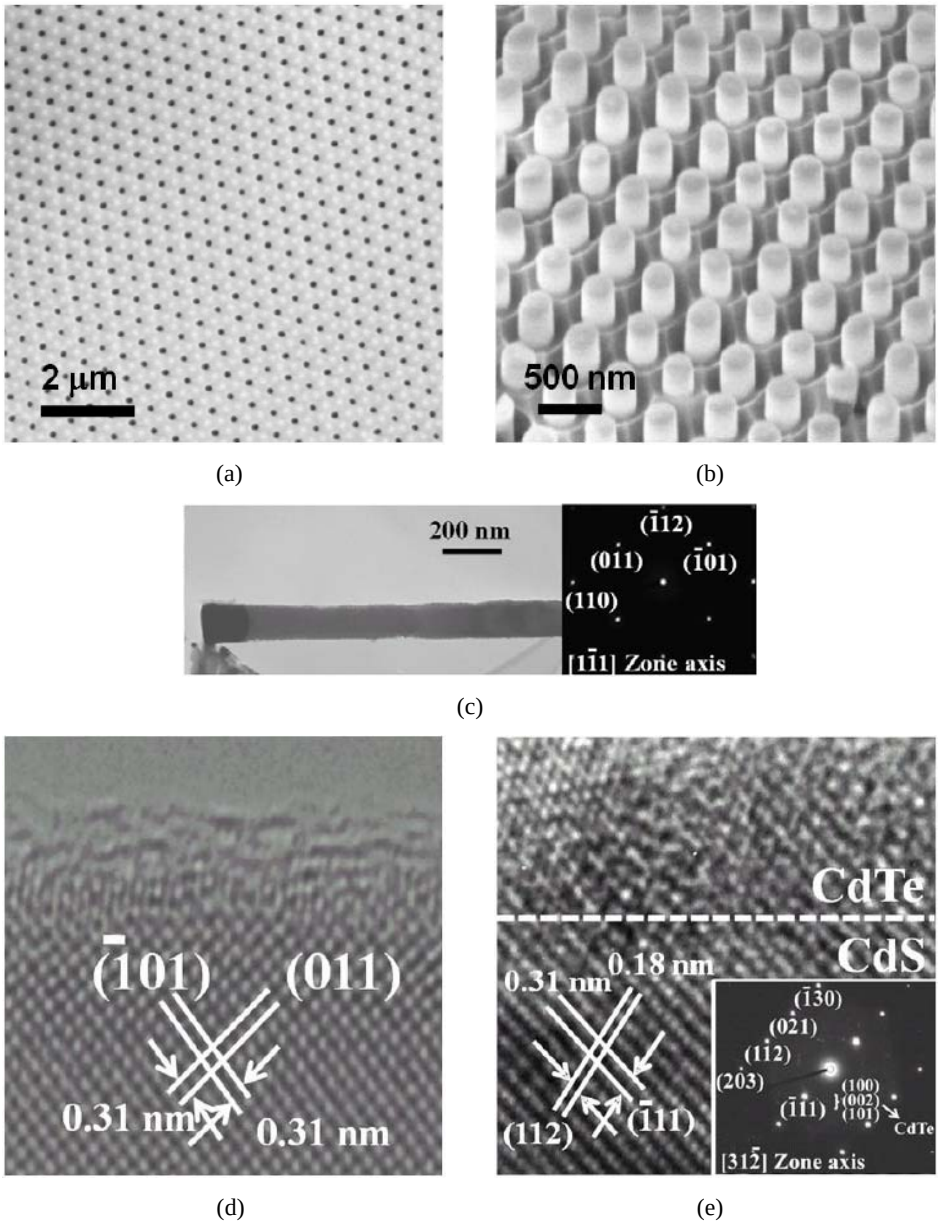

Source: Reprinted with permission from Fan et al. (2009)

In order to demonstrate the capability of fabricating single-crystalline NPL arrays on an amorphous substrate with the fine geometric control without relying on the epitaxial growth from single-crystalline substrates, single-crystalline structure of CdS NPLs was

confirmed by the low-resolution and high-resolution TEM in Figure 6(c) and Figure 6(d), respectively. More importantly, Figure 6(e) shows the abrupt junction between the CdS NPLs and the CdTe film which is essential for the efficient photo-carrier separation. An excellent junction or interface quality can minimise the photogenerated carrier loss through the non-radiative recombination at the defect sites (Czaban et al., 2009; Tsakalakos et al., 2007).

Figure 7 CdS NPL/CdTe thin film PVs (a) an optical image of a fully fabricated cell bonded to a glass substrate (b) *I-V* characteristics under various illumination conditions (c) conversion efficiency, η, and open circuit voltage, V_{oc}, as a function of illumination intensity (see online version for colours)

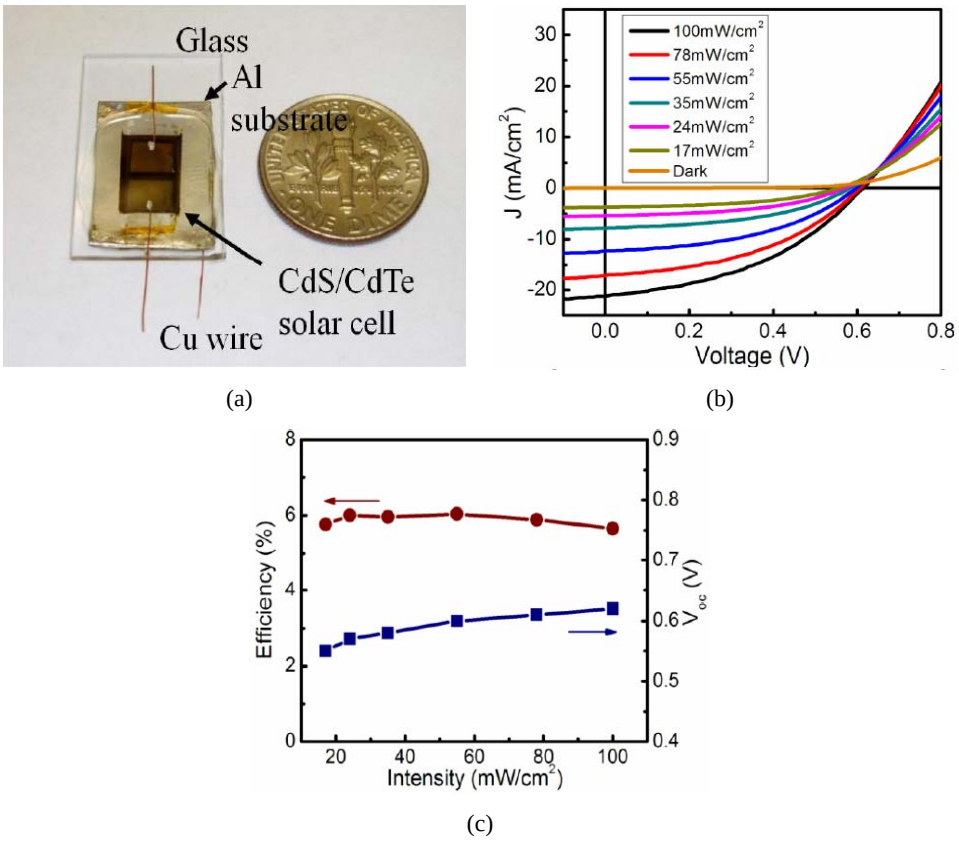

(a) (b)

(c)

Source: Reprinted with permission from Fan et al. (2009)

A photograph of a fully fabricated SNOP cell device is shown in Figure 7(a) where the device has an active surface area of 5 mm × 8 mm. The cell performance was assessed by utilising a solar simulator (LS1000, solar light) without a heat sink and the current-voltage (I-V) characteristics of a typical cell under different illumination intensities, P, ranging from dark to 100 mWcm^2 (AM 1.5G), was shown in Figure 7(b). Under AM 1.5G illumination, the cell produced a short circuit current density (J_{SC}) of ~21 mA cm^{-2}, a open circuit voltage (V_{OC}) of ~0.62 V and a fill factor (FF) of ~43%. An efficiency (η) of ~6% was reported in Figure 7(c) which is mostly restricted by the inadequate optical transmission of the top metal contact and the absence of anti-reflection coating. The I-V

curves cross over each other above V_{OC} which can be attributed to the photoconductivity of CdS (Corwine et al., 2004). The dependency of V_{OC} on the illumination intensity is shown in Figure 7(c). Voc only increases slightly from 0.55 to 0.62 V with a linear increase of Jsc, which can be attributed to a slight thermal heating of the device since a cooling chuck was not utilised in the measurements (Sze, 1981).

The SNOP cells reported here already have the energy conversion efficiency higher than most of the previously reported PVs based on nanostructured materials; (Czaban et al., 2009; Garnett and Yang, 2008; Tsakalakos et al., 2007) however, more detailed investigations are still in process to enhance the efficiency to meet the high-performance application requirements. Notably, the reported efficiency is higher than that of the planar CdS/CdTe cell with the comparable CdTe film thickness, (Marsillac et al., 2007) but still lowers than those with optimal CdTe film thicknesses. In future, the cell efficiency can be readily improved through the further device and materials optimisation as confirmed by the simulation. For example, utilising top electrical contacts with higher optical transparency and lower parasitic resistances, the efficiency can be easily boosted up to > 10% (Kapadia et al. 2010).

Another key advantage of this 3D SNOP cell over other conventional cell structures relies on the geometrical configuration (vertical regular arrays arrangement) for the improved carrier collection efficiency. As expected, the conversion efficiency drastically and monotonically increases with the NPL embedded height (H) in CdTe film. Specifically, η is ~0.4% for the case of H = 0 nm that only the top surface of the CdS NPLs is in contact with the CdTe film; therefore, a small space charge region for the carrier collection is resulted in the low conversion efficiency. On the other hand, increasing H, the space charge region area is increased accordingly to enhance the carrier collection efficiency. In particular, the device conversion efficiency is raised by more than one order of magnitude when H is increased from 0 to ~640 nm. All these results clearly indicate the benefit of this 3D structure and put forward a future route to improve the cell performance by optimising the geometric design of device structures. However, as discussed in the previous session, the SNOP cell structure may only be advantageous as compared with conventional planar-structured PVs if the interface recombination is not the limiting factor for cell performance; for that reason, this 3D cell structure requires a careful material system consideration for the carrier loss dominating by the bulk recombination processes as oppose to the surface or interface/junction recombination.

In addition to the rigid substrates, this SNOP cell fabrication scheme can also be applied on the bendable plastics for flexible and high performance PVs, which are of particular interest for a number of technological applications (Yoon et al., 2008; Fan and Javey, 2008; Lungenschmied et al., 2007) Simply, a layer of polydimethylsiloxane (PDMS, ~2 mm thick) is deposited and cured on the top surface following the top-contact metallisation process. Then the aluminium substrate at the back is released by a wet chemical etching process. A layer of ~200 nm thick indium film is deposited as the bottom contact to the n-CdS NPLs and another ~2 mm thick PDMS layer is put down and cured on the back side to complete the encapsulation. In this case, as shown in the optical image and device structural schematic in Figure 8(a), the entire SNOP cell is sandwiched and embedded within the flexible and bendable plastic materials. Notably, the entire SNOP cell structure is located in the neutral mechanical plane of the PDMS substrate which minimises the strain on the active cell elements, CdS NPLs. Verified by the strain simulation, when the plastic encapsulated SNOP cell is bended to a 3 cm radius of

curvature, this induces a maximum 8% of tensile and compressive strain on the top and bottom surfaces of the ~4 mm thick PDMS substrate, respectively, while the NPLs in ~2 μm in height would only experience a maximum of ~0.01% strain (Fan et al., 2009). Figure 8(b) demonstrates the I-V characteristics of a plastic SNOP module under different bending conditions and confirms the negligible change in the cell performance such as the energy conversion efficiency upon bending within the given bending radius down to 27 mm. All these results suggest that this flexible SNOP PV structure can withstand a large amount of bending without any significant structural and performance degradation, which reveal the potency for flexible solar cell applications.

Figure 8 Mechanically flexible CdS NPLs/CdTe thin film PVs (a) an optical image and schematic (inert) of a bendable module embedded in PDMS (b) *I-V* characteristics of a flexible cell for various bending radii, showing minimal dependence on curvature (see online version for colours)

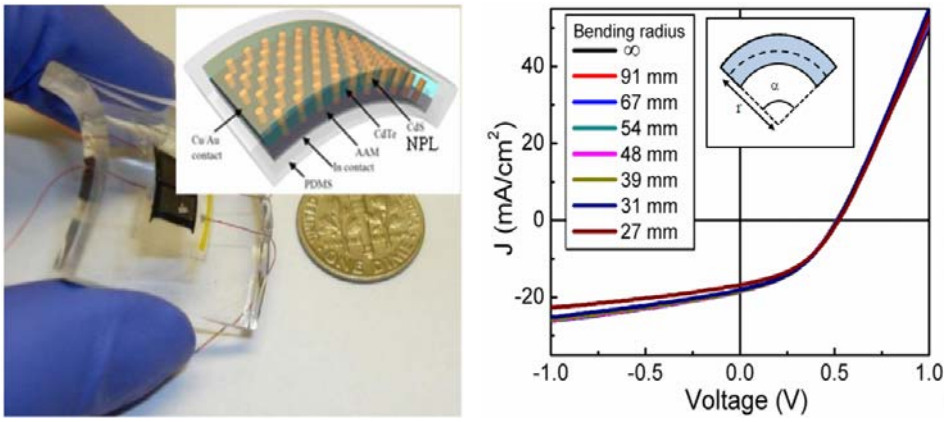

(a) (b)

Source: Reprinted with permission from Fan et al. (2010)

Again, the ability to directly grow single-crystalline active material structures on large aluminium sheets here is highly attractive to minimise the materials and processing costs. Also, this 3D cell configuration can relax the materials requirements in terms of quality and purity which can further lower the costs. However, further exploration of various low-cost and conductive film deposition processes, such as top-contact ink jet printing, are still needed to further enhance the versatility and lower the cost of this proposed solar modules.

6 Conclusions

Significant progress has been made continuously on PV devices using 1D nanostructures. As discussed in this review article, forming 3D PV architectures with 1D materials can significant improve the light absorption and carrier collection. In particular, the enhancement of light absorption for a 3D nanostructure can be largely engineered, simply with a low-cost bottom-up synthetic approach. This is a significant break-through for PV technologies since in which cost is one of the primary concerns. On the other hand, it is

important to point out that not all conventional PV materials are good for nanostructured solar cells, mainly due to the large surface area of the structures. It is conceivable that materials systems with high surface recombination velocity (SRV), such as Si, GaAs, etc., are not ideal materials for nanostructured PV while materials with low SRV, e.g., CdTe/CdS, are suitable for making efficient nanostructured PV. In such a context, NPL CdS/thin film CdTe PV devices have been demonstrated, with a respectable efficiency. More importantly, the demonstrated fabrication processes meet the requirements of scalability, low cost and flexibility. With further improved performance, this technology can be one of the promising candidates for next generation PVs.

Acknowledgements

Z. Fan acknowledges the support from the HKUST (Project No.: DAG.09/10.EG09). J.C. Ho acknowledges the support from City University of Hong Kong (Project No. 7200203 and 7002597).

References

Bandaranayake, K.M.P., Senevirathna, M.K.I., Weligamuwa, P.M.G.M.P. and Tennakone, K. (2004) 'Dye-sensitized solar cells made from nanocrystalline TiO2 films coated with outer layers of different oxide materials', *Coordination Chemistry Reviews*, Vol. 248, Nos. 13–14, pp.1277–1281.

Bullis, W.M. (1966) 'Properties of gold in silicon', *Solid State Electronics*, Vol. 9, pp.143–168.

Chen, P., Shen, G. and Zhou, C. (2008) 'Chemical sensors and electronic noses based on 1-D metal oxide nanostructures', *IEEE Transactions on Nanotechnology*, Vol. 7, No. 6, pp.668–682.

Colombo, C., Heiss, M., Gratzel, M. and Morral, A.F.I. (2009) 'Gallium arsenide p-i-n radial structures for photovoltaic applications', *Applied Physics Letters*, Vol. 94, No. 17, p.173108.

Corwine, C.R., Pudov, A.O., Gloeckler, M., Demtsu, S.H. and Sites, J.R. (2004) 'Copper inclusion and migration from the back contact in CdTe solar cells', *Solar Energy Materials and Solar Cells*, Vol. 82, No. 4, pp.481–489.

Czaban, J.A., Thompson, D.A. and LaPierre, R.R. (2009) 'GaAs core-shell nanowires for photovoltaic applications', *Nano Letters*, Vol. 9, No. 1, pp.148–154.

Delgadillo, I., Vargas, M., CruzOrea, A., AlvaradoGil, J.J., Baquero, R., SanchezSinencio, F. and Vargas, H. (1997) 'Photoacoustic CdTe surface characterization', *Applied Physics B – Lasers and Optics*, Vol. 64, No. 1, pp.97–101.

Diamant, Y., Chappel, S., Chen, S.G., Melamed, O. and Zaban, A. (2004) 'Core-shell nanoporous electrode for dye sensitized solar cells: the effect of shell characteristics on the electronic properties of the electrode', *Coordination Chemistry Reviews*, Vol. 248, Nos. 13–14, pp.1271–1276.

Fahrenbruch, A.L. and Bube, R.H. (1983) *Fundamentals of Solar Cells: Photovoltaic Solar Energy Conversion*, Academic Press, Inc., New York.

Fan, Z. and Javey, A. (2008) 'Solar cells on curtains', *Nature Materials*, Vol. 7, No. 11, p.835.

Fan, Z.Y., Chang, P.C., Lu, J.G., Walter, E.C., Penner, R.M., Lin, C.H. and Lee, H.P. (2004a) 'Photoluminescence and polarized photodetection of single ZnO nanowires', *Applied Physics Letters*, Vol. 85, No. 25, pp.6128–6130.

Fan, Z.Y., Wang, D.W., Chang, P.C., Tseng, W.Y. and Lu, J.G. (2004b) 'ZnO nanowire field-effect transistor and oxygen sensing property', *Applied Physics Letters*, Vol. 85, No. 24, pp.5923–5925.

Fan, Z.Y., Ho, J.C., Jacobson, Z.A., Razavi, H. and Javey, A. (2008a) 'Large-scale, heterogeneous integration of nanowire arrays for image sensor circuitry', *Proceedings of the National Academy of Sciences of the United States of America*, Vol. 105, No. 32, pp.11066–11070.

Fan, Z.Y., Ho, J.C., Jacobson, Z.A., Yerushalmi, R., Alley, R.L., Razavi, H. and Javey, A. (2008b) 'Wafer-scale assembly of highly ordered semiconductor nanowire arrays by contact printing', *Nano Letters*, Vol. 8, No. 1, pp.20–25.

Fan, Z.Y. and Lu, J.G. (2005) 'Gate-refreshable nanowire chemical sensors', *Applied Physics Letters*, Vol. 86, No. 12, p.123510.

Fan, Z.Y., Razavi, H., Do, J.W., Moriwaki, A., Ergen, O., Chueh, Y.L., Leu, P.W., Ho, J.C., Takahashi, T., Reichertz, L.A., Neale, S., Yu, K., Wu, M., Ager, J.W. and Javey, A. (2009) 'Three-dimensional nanopillar-array photovoltaics on low-cost and flexible substrates', *Nature Materials*, Vol. 8, No. 8, pp.648–653.

Fan, Z., Kapadia, R., Leu, P.W., Zhang, X., Chueh, Y., Takei, K., Yu, K., Jamshidi, A., Rathore, A.A., Ruebusch, D.J., Wu, M. and Javey, A. (2010) 'Ordered arrays of dual-diameter nanopillars for maximized optical absorption', *Nano Letters*.

Ford, A.C., Ho, J.C., Chueh, Y.L., Tseng, Y.C., Fan, Z.Y., Guo, J., Bokor, J. and Javey, A. (2009) 'Diameter-dependent electron mobility of InAs nanowires', *Nano Letters*, Vol. 9, No. 1, pp.360–365.

Garnett, E.C. and Yang, P.D. (2010) 'Light trapping in silicon nanowire solar cells', *Nano Letters*, ASAP.

Garnett, E.C. and Yang, P.D. (2008) 'Silicon nanowire radial p-n junction solar cells', *Journal of the American Chemical Society*, Vol. 130, No. 29, pp.9224–9225.

Greene, L.E., Law, M., Yuhas, B.D. and Yang, P.D. (2007) 'ZnO-TiO2 core-shell nanorod/P3HT solar cells', *Journal of Physical Chemistry C*, Vol. 111, No. 50, pp.18451–18456.

Hahm, J. and Lieber, C.M. (2004) 'Direct ultrasensitive electrical detection of DNA and DNA sequence variations using nanowire nanosensors', *Nano Letters*, Vol. 4, No. 1, pp.51–54.

Hasegawa, Y., Murata, M., Nakamura, D. and Komine, T. (2009) 'Reducing thermal conductivity of thermoelectric materials by using a narrow wire geometry', *Journal of Applied Physics*, Vol. 106, No. 6, p.063703.

Hochbaum, A.I., Chen, R.K., Delgado, R.D., Liang, W.J., Garnett, E.C., Najarian, M., Majumdar, A. and Yang, P.D. (2008) 'Enhanced thermoelectric performance of rough silicon nanowires', *Nature*, Vol. 451, No. 7175, pp.163–168.

Hu, L. and Chen, G. (2007) 'Analysis of optical absorption in silicon nanowire arrays for photovoltaic applications', *Nano Letters*, Vol. 7, pp.3249–3252.

Jastrzebski, L., Lagowski, J. and Gatos, H.C. (1975) 'Application of scanning electron-microscopy to determination of surface recombination velocity – GaAs', *Applied Physics Letters*, Vol. 27, No. 10, pp.537–539.

Javey, A. (2008) 'The 2008 Kavli Prize in nanoscience: carbon nanotubes', *Acs. Nano*, Vol. 2, No. 7, pp.1329–1335.

Javey, A., Nam, S., Friedman, R.S., Yan, H. and Lieber, C.M. (2007) 'Layer-by-layer assembly of nanowires for three-dimensional, multifunctional electronics', *Nano Letters*, Vol. 7, No. 3, pp.773–777.

Kapadia, R., Fan, Z. and Javey, A. (2010) 'Design constraints and guidelines for CdS/CdTe nanopillar based photovoltaics', *Applied Physics Letters*, Vol. 96, No. 10, p.103116.

Kayes, B.M., Atwater, H.A. and Lewis, N.S. (2005) 'Comparison of the device physics principles of planar and radial p-n junction nanorod solar cells', *Journal of Applied Physics*, Vol. 97, p.114302.

Kelzenberg, M.D., Turner-Evans, D.B., Kayes, B.M., Filler, M.A., Putnam, M.C., Lewis, N.S. and Atwater, H.A. (2008) 'Photovoltaic measurements in single-nanowire silicon solar cells', *Nano Letters*, Vol. 8, No. 2, pp.710–714.

Kelzenberg, M.D., Boettcher, S.W., Petykiewicz, J.A., Turner-Evans, D.B., Putnam, M.C., Warren, E.L., Spurgeon, J.M., Briggs, R.M., Lewis, N.S. and Atwater, H.A. (2010) 'Enhanced absorption and carrier collection in Si wire array for photovoltaic applications', *Nature Materials*, Advanced Online Publication.

Kempa, T.J., Tian, B., Kim, D.R., Hu, J., Zheng, X. and Lieber, C.M. (2008) 'Single and tandem axial p-i-n nanowire photovoltaic devices', *Nano Letters*, Vol. 8, No. 10, pp.3456–3460.

Law, M., Greene, L.E., Johnson, J.C., Saykally, R. and Yang, P.D. (2005) 'Nanowire dye-sensitized solar cells', *Nature Materials*, Vol. 4, No. 6, pp.455–459.

Law, M., Greene, L.E., Radenovic, A., Kuykendall, T., Liphardt, J. and Yang, P.D. (2006) 'ZnO-Al2O3 and ZnO-TiO2 core-shell nanowire dye-sensitized solar cells', *Journal of Physical Chemistry B*, Vol. 110, No. 45, pp.22652–22663.

Lu, W. and Lieber, C.M. (2007) 'Nanoelectronics from the bottom up', *Nature Materials*, Vol. 6, pp.841–850.

Lungenschmied, C., Dennler, G., Neugebauer, H., Sariciftci, S.N., Glatthaar, M., Meyer, T. and Meyer, A. (2007) 'Flexible, long-lived, large-area, organic solar cells', *Solar Energy Materials and Solar Cells*, Vol. 91, No. 5, pp.379–384.

Marsillac, S., Parikh, V.Y. and Compaan, A.D. (2007) 'Ultra-thin bifacial CdTe solar cell', *Solar Energy Materials and Solar Cells*, Vol. 91, Nos. 15–16, pp.1398–1402.

Martinson, A.B.F., Elam, J.W., Liu, J., Pellin, M.J., Marks, T.J. and Hupp, J.T. (2008) 'Radial electron collection in dye-sensitized solar cells', *Nano Letters*, Vol. 8, No. 9, pp.2862–2866.

Masuda, H., Yamada, H., Satoh, M., Asoh, H., Nakao, M. and Tamamura, T. (1997) 'Highly ordered nanochannel-array architecture in anodic alumina', *Applied Physics Letters*, Vol. 71, No. 19, pp.2770–2772.

Mikulskas, I., Juodkazis, S., Tomasiunas, R. and Dumas, J.G. (2001) 'Aluminum oxide photonic crystals grown by a new hybrid method', *Advanced Materials*, Vol. 13, No. 20, pp.1574–1577.

Mohammad, S.N. (2009) 'For nanowire growth, vapor-solid-solid (vapor-solid) mechanism is actually vapor-quasisolid-solid (vapor-quasiliquid-solid) mechanism', *Journal of Chemical Physics*, Vol. 131, No. 22.

Muskens, O.L., Rivas, J.G., Algra, R.E., Bakkers, E.P.A.M. and Lagendijk, A. (2008) 'Design of light scattering in nanowire materials for photovoltaic applications', *Nano Letters*, Vol. 8, No. 9, pp.2638–2642.

Palomares, E., Clifford, J.N., Haque, S.A., Lutz, T. and Durrant, J.R. (2003) 'Control of charge recombination dynamics in dye sensitized solar cells by the use of conformally deposited metal oxide blocking layers', *Journal of the American Chemical Society*, Vol. 125, No. 2, pp.475–482.

Passlack, M., Hong, M., Mannaerts, J.P., Kwo, J.R. and Tu, L.W. (1996) 'Recombination velocity at oxide-GaAs interfaces fabricated by in situ molecular beam epitaxy', *Applied Physics Letters*, Vol. 68, No. 25, pp.3605–3607.

Qian, F., Gradecak, S., Li, Y., Wen, C.Y. and Lieber, C.M. (2005) 'Core/multishell nanowire heterostructures as multicolor, high-efficiency light-emitting diodes', *Nano Letters*, Vol. 5, No. 11, pp.2287–2291.

Rosenwaks, Y., Burstein, L., Shapira, Y. and Huppert, D. (1990) 'Effects of reactive versus unreactive metals on the surface recombination velocity at Cds and Cdse (1120) interfaces', *Applied Physics Letters*, Vol. 57, No. 5, pp.458–460.

Rowe, M.W., Liu, H.L., Williams, G.P. and Williams, R.T. (1993) 'Picosecond photoelectron-spectroscopy of excited-states at Si(111) root-3 X root-3r 30-degrees-B, Si(111)7x7, Si(100)2x1, and laser-annealed Si(111)1x1 surfaces', *Physical Review B*, Vol. 47, No. 4, pp.2048–2064.

Sabbah, A.J. and Riffe, D.M. (2000) 'Measurement of silicon surface recombination velocity using ultrafast pump-probe reflectivity in the near infrared', *Journal of Applied Physics*, Vol. 88, No. 11, pp.6954–6956.

Sharma, A.K., Agarwal, S.K. and Singh, S.N. (2007) 'Determination of front surface recombination velocity of silicon solar cells using the short-wavelength spectral response', *Solar Energy Materials and Solar Cells*, Vol. 91, Nos. 15–16, pp.1515–1520.

Song, M.Y., Ahn, Y.R., Jo, S.M., Kim, D.Y. and Ahn, J.P. (2005) 'TiO2 single-crystalline nanorod electrode for quasi-solid-state dye-sensitized solar cells', *Applied Physics Letters*, Vol. 87, No. 11, p.113113.

Spurgeon, J.M., Atwater, H.A. and Lewis, N.S. (2008) 'A comparison between the behavior of nanorod array and planar Cd(Se, Te) photoelectrodes', *Journal of Physical Chemistry C*, Vol. 112, No. 15, pp.6186–6193.

Stiebig, H., Senoussaoui, N., Zahren, C., Haase, C. and Muller, J. (2006) 'Silicon thin-film solar cells with rectangular-shaped grating couplers', *Progress in Photovoltaics*, Vol. 14, No. 1, pp.13–24.

Sze, S.M. (Ed.) (1981) *Physics of Semiconductor Devices*, 2nd ed., Wiley-Interscience Publication, New York.

Tang, Y.B., Chen, Z.H., Song, H.S., Lee, C.S., Cong, H.T., Cheng, H.M., Zhang, W.J., Bello, I. and Lee, S.T. (2008) 'Vertically aligned p-type single-crystalline GaN nanorod arrays on n-type Si for heterojunction photovoltaic cells', *Nano Letters*, Vol. 8, pp.4191–4195.

Tennakone, K., Bandara, J., Bandaranayake, P.K.M., Kumara, G.R.A. and Konno, A. (2001) 'Enhanced efficiency of a dye-sensitized solar cell made from MgO-coated nanocrystalline SnO2', *Japanese Journal of Applied Physics Part 2 – Letters*, Vol. 40, No. 7B, pp.L732–L734.

Thelander, C., Rehnstedt, C., Froberg, L.E., Lind, E., Martensson, T., Caroff, P., Lowgren, T., Ohlsson, B.J., Samuelson, L. and Wernersson, L.E. (2008) 'Development of a vertical wrap-gated InAs FET', *IEEE Transactions on Electron Devices*, Vol. 55, No. 11, pp.3030–3036.

Tian, B.Z., Zheng, X.L., Kempa, T.J., Fang, Y., Yu, N.F., Yu, G.H., Huang, J.L. and Lieber, C.M. (2007) 'Coaxial silicon nanowires as solar cells and nanoelectronic power sources', *Nature*, Vol. 449, pp.885–889.

Tsakalakos, L., Balch, J., Fronheiser, J., Korevaar, B.A., Sulima, O. and Rand, J. (2007) 'Silicon nanowire solar cells', *Applied Physics Letters*, Vol. 91, No. 233117.

Wang, D. and Dai, H. (2006) 'Germanium nanowires: from synthesis, surface chemistry, and assembly to devices', *Applied Physics A – Materials Science & Processing*, Vol. 85, No. 3, pp.217–225.

Wang, Y.W., Schmidt, V., Senz, S. and Gosele, U. (2006) 'Epitaxial growth of silicon nanowires using an aluminium catalyst', *Nature Nanotechnology*, Vol. 1, No. 3, pp.186–189.

Wang, Z.L. and Song, J.H. (2006) 'Piezoelectric nanogenerators based on zinc oxide nanowire arrays', *Science*, Vol. 312, No. 5771, pp.242–246.

Xiang, J., Lu, W., Hu, Y.J., Wu, Y., Yan, H. and Lieber, C.M. (2006) 'Ge/Si nanowire heterostructures as high-performance field-effect transistors', *Nature*, Vol. 441, No. 7092, pp.489–493.

Yoon, J., Baca, A.J., Park, S., Elvikis, P., Geddes, J.B., Li, L., Kim, R.H., Xiao, J., Wang, S., Kim, T.-, Motala, M.J., Ahn, B.Y., Duoss, E.B., Lewis, J.A., Nuzzo, R.G., Ferreir, P.M., Huang, Y., Rockett, A. and Rogers, J.A. (2008) 'Ultrathin silicon solar microcells for semitransparent, mechanically flexible and microconcentrator module designs', *Nature Materials*, Vol. 7, No. 11, pp.907–915.

Zaban, A., Chen, S.G., Chappel, S. and Gregg, B.A. (2000) 'Bilayer nanoporous electrodes for dye sensitized solar cells', *Chemical Communications*, No. 22, pp.2231–2232.

Zhang, D.H., Liu, Z.Q., Li, C., Tang, T., Liu, X.L., Han, S., Lei, B. and Zhou, C.W. (2004) 'Detection of NO2 down to ppb levels using individual and multiple In2O3 nanowire devices', *Nano Letters*, Vol. 4, No. 10, pp.1919–1924.

Zhong, Z.H., Qian, F., Wang, D.L. and Lieber, C.M. (2003) 'Synthesis of p-type gallium nitride nanowires for electronic and photonic nanodevices', *Nano Letters*, Vol. 3, No. 3, pp.343–346.

Zhu, J., Yu, Z.F., Burkhard, G.F., Hsu, C.M., Connor, S.T., Xu, Y.Q., Wang, Q., McGehee, M., Fan, S.H. and Cui, Y. (2009) 'Optical absorption enhancement in amorphous silicon nanowire and nanocone arrays', *Nano Letters*, Vol. 9, No. 1, pp.279–282.